Vol. 86 (1994) ACTA PHYSICA POLONICA A No. 5

Proceedings of the ISSSRNS '94, Jaszowiec 1994

OXYGEN AND SILICON K-EXAFS IN SiO_2

R. NIETUBYĆ

Institute of Physics, Polish Academy of Sciences
Al. Lotników 32/46, 02-668 Warszawa, Poland

The aim of this work was to calculate EXAFS (extended X-ray absorption fine structure) profile of the constituent elements for SiO_2 in β-quartz and in its amorphous form within a single scattering curved waves approximation. This method extends the EXAFS analysis to lower energies than the plane wave approximation. We have used wave functions for free ions and Pendry's procedure for central atom phase shifts calculation. Our results for Si K-EXAFS were consistent with experiment, whereas a significant deviation from experimental results for O K-EXAFS was observed. Similar EXAFS profiles for β-quartz and amorphous SiO_2 were obtained from calculations.

PACS numbers: 61.10.Wg, 78.70.Dm

1. Introduction

EXAFS is a good technique for investigation of the local structure around absorbing elements, for example in glasses [1, 2], but also in more complicated compounds like high temperature superconductors [3, 4]. Tabulated data of phase shifts [5, 6] are usually used for EXAFS single scattering simulation, however many authors calculate phase shifts by themselves in a single [7] and multiple [8, 9] scattering approach.

The X-ray photoabsorption process consists in an ejection of an electron from an atomic core level. The absorption coefficient, when the atom is located in a molecule or solid, is modified comparatively to the free atom process and the oscillation function $\chi(k)$ appears as

$$\chi(k) = \frac{\mu - \mu_0}{\mu_0}, \tag{1}$$

where χ — EXAFS oscillating function, μ — absorption coefficient, μ_0 — atomic absorption coefficient [10].

Our aim was to calculate EXAFS oscillations for SiO_2, i.e. β-quartz and its amorphous form. We decided to calculate the central atom phase shifts and backscattering functions because the application of literature data [5, 6, 11] gave the results significantly different from experiment [12, 13]. Our approach is based

on the following approximations: muffin-tin potential and curved waves single scattering [5, 14, 15], it enables us to obtain results for energy region extended from 30 eV above the absorption edge.

2. Theory

From the single scattering theory of EXAFS [16] the K-EXAFS oscillations are described by the following formula:

$$\chi(k) = -\sum_j \frac{N_j}{kr_j^2} |f_j(k,\pi)| \exp(-2\sigma_j^2 k^2) \exp\left[-2r_j\left(\frac{1}{\lambda_f} + \frac{1}{\lambda_h}\right)\right] \times \sin(2kr_j + 2\delta + \theta_j), \tag{2}$$

where j — index numbering neighbor shell, N_j — neighbor shell occupation, f_j — backscattering amplitude, r_j — shell radius, δ — central atom phase shift, θ_j — phase of backscattering function for $l = 1$, λ_f — mean free path of electron associated with inelastic scattering, λ_h — mean free path of electron associated with K-hole lifetime, k — electron momentum, σ_j — Debye–Waller factor.

A single scattering approximation means that we take into account only a contribution from events of electron propagation from a central atom to a neighbor and back. A curved waves approximation is consistent with treating a scattering process as it occurs in the close neighborhood of central atom where the electron wave is represented by a spherical wave centered on the absorber and having respectively to this point a well-defined angular momentum number. In this approximation the backscattering function for $l = 1$ is calculated by using the following formula from Ref. [5]:

$$f_j(k, r_j) = |f_j(k, r_j)| \exp[i\theta_j(k, r_j)]$$

$$= \frac{kr_j^2}{\exp(2ikr_j)} \sum_{l'} (2l'+1)(-1)^{l'} \exp(i\delta_{l'}) \sin\delta_{l'} \left\{ \frac{l'+1}{2l'+1} [h^+_{l'+1}(kr_j)]^2 + \frac{l'-1}{2l'+1} [h^+_{l'-1}(kr_j)]^2 \right\}, \tag{3}$$

where $h_{l'}$ is a Hankel function of l' range. This formula points out the difference between the curved and plane wave approximation.

Physical meaning of the curved wave approach is that it is sensitive to the curvature of a wave representing electron. In opposition to the plane wave approach, such a model gives better results if we consider backscattering on close neighbors, or in low energy region. In these cases the size of backscatterer cannot be neglected. From the mathematical point of view a curved wave approaches a plane wave when the Hankel function can be replaced by its asymptotic form in the high energy limit

$$i^l h_l(kr) \approx \frac{e^{ikr}}{ikr}. \tag{4}$$

It is seen that the region of the plane wave approximation is determined by a product of momentum and distance. If we consider for SiO_2 a condition presented in Ref. [15], we can estimate that an effect of curvature is smaller than 10% for energies above 60 eV.

3. Data and treatment

There exist many different forms of SiO_2. We have chosen β-quartz and amorphous SiO_2 as a model material. β-quartz, formed from α-quartz by heat treatment at 840 K, was chosen due to its high symmetry. The nearest neighbor order around Si^{+4} and O^{-2} ions is similar in all crystalline SiO_2 forms, where there are tetrahedra with an almost constant length of Si–O bond equal to about 1.6 Å. Tetrahedra orientation and construction are slightly differentiated, in amorphous SiO_2, it means that bond lengths and Si–O–Si angles are not constant all over the sample.

We construct an amorphous model taking interatomic distances characteristic of β-quartz and assuming Debye–Waller factor as a progressing function of neighbor shell radius. Its value has a range from 0.1 to 0.25 Å. Such a model does not take into account neither defects nor the deviations from the stoichiometric formula. The radial distribution function (RDF) obtained from our structure model for amorphous silicon dioxide was compared with the data presented in literature [17, 18] (see Fig. 1). It can be seen that the distribution of density between the observed maxima is different (X-ray scattering RDF is presented in Ref. [17]), but the positions of the maxima are the same. According to the formula (2) we expect that for amorphous SiO_2 only three nearest shells give essential contributions to K-EXAFS, whereas the influence of the rest is reduced by inelastic scattering and structure disorder.

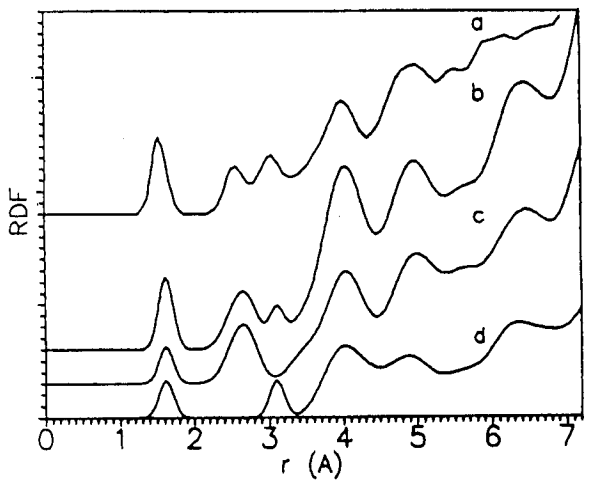

Fig. 1. Radial distribution functions: *a* — for X-ray scattering given by W.Y. Ching [17], *b* — our amorphous model, *c* — our amorphous model — partial contribution around O atom, *d* — our amorphous model — partial contribution around Si atom.

Dumping of the $\chi(k)$ (see Eq. (2)) is mathematically described by exponential factors: the first is associated with Debye–Waller factor which describes temperature and structural disorder, the second one is connected with inelastic

scattering and core–hole lifetime. These factors decrease the EXAFS oscillations amplitude with increase in neighbor shell radius and photoelectron energy.

Central atom phase shifts were calculated on the basis of free atomic wave function for O^{-2} (two valence electrons were added to a neutral atom to obtain an ion wave function), and Si^{+4} ions [19]. We have used Pendry's procedure for the central atom phase shift calculation in Hartree–Fock and muffin-tin approximations [20]. The partial phase shifts are input data to backscattering amplitude calculations (see Eq. (3)). We have compared central atom phase shifts obtained by us with the results presented in literature [6] and we found an agreement between them for the momentum higher than 4 $Å^{-1}$ (equivalent to the energy 60 eV) (see Fig. 2). Backscattering phase shifts, calculated here, were compared with the data of [5, 11] and differences were observed for Si, while for O our data were in agreement with the ones of Ref. [5].

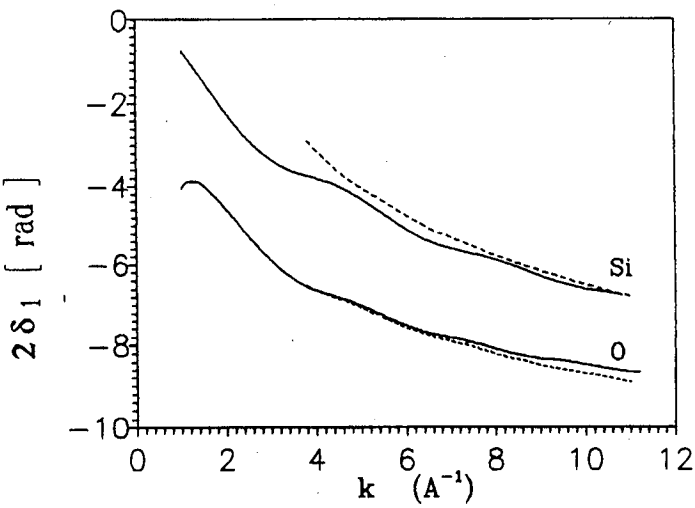

Fig. 2. Central atom phase shifts $l = 1$, for Si and O. Dotted line — Teo and Lee data [6], solid line — our calculations.

4. Results

We present the results of our EXAFS simulations for amorphous form of SiO_2 in Fig. 3 and for β-quartz in Fig. 4. Si K-EXAFS (curve g in Fig. 3) obtained from our phase shifts calculation is in good agreement with the experimental result [13]. The role of oxygen neighbor shells is dominant, the most important of them is the first one (r = 1.61 Å). Oscillations provided by silicon shells disappear above 50 eV for both β-quartz and amorphous form.

It can be easily seen (Fig. 3 and Table I) that Si K-EXAFS profile calculated by using our phase shifts and amplitudes are more conformable with experiment than the profiles obtained on the basis of the tabulated data [5, 6, 11]. The tabulated data lead to the profiles which are in an opposite phase as compared to the

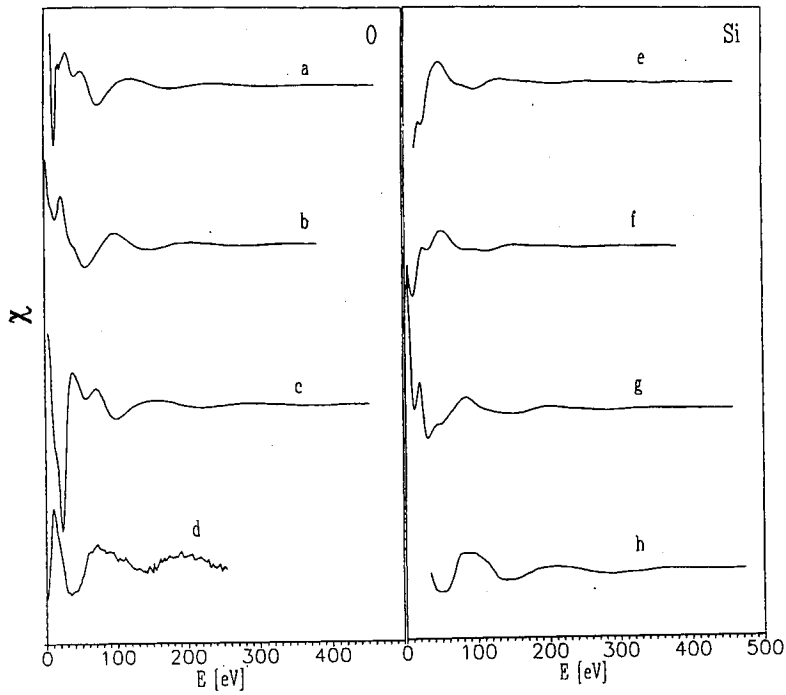

Fig. 3. O K-EXAFS and Si K-EXAFS for amorphous silicon dioxide: a, e — calculated on the basis of central atom phase shifts given by Teo and Lee [6] and backscattering functions given by Mc Kale et al. [5], b, f — calculation on the basis of central atom phase shifts and backscattering amplitude given by Mustre de Leon et al. [11], c, g — our results, d — experimental result [12] for oxygen, h — experimental result [13] for silicon.

experimentally observed ones. The positions of maxima and minima of our and experimental Si K-EXAFS profiles are in agreement within 10 eV (Table I).

For O K-EXAFS, comparing with the results obtained from the tabulated data any significant progress has been reached. Our profile is different than those obtained from the tabulated data and different from the experimental one [12].

The agreement of the O K-EXAFS profile calculated by us (curve c in Fig. 3) with the experimental one will be better if we shift down the muffin-tin zero energy by 30 eV. Contributions to $\chi(k)$ arising from Si and O neighbor shells were analyzed. We have noticed that O K-EXAFS spectrum below 100 eV is a sum of approximately equal contributions originating from scattering by both O and Si elements. The dominant influence of the Si 1.61 Å shell can be seen above 100 eV. A small difference between EXAFS profiles for amorphous SiO_2 and β-quartz can be seen in Fig. 4. Fast varying oscillations provided by long distance shells appear only in β-quartz profiles, while they are dumped in amorphous form one.

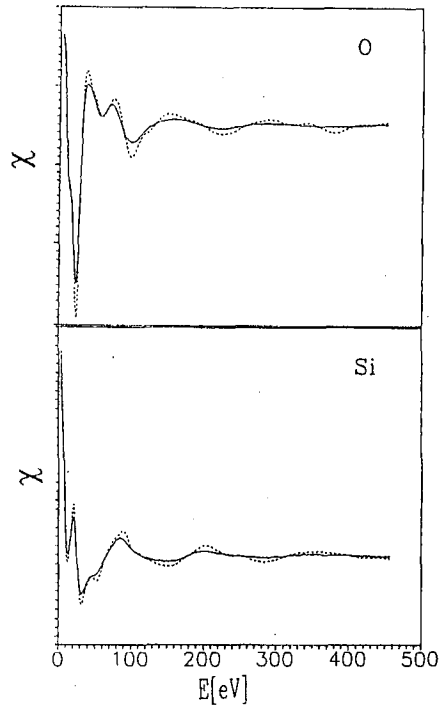

Fig. 4. K-EXAFS, comparison between β-quartz (dotted line) and amorphous silicon dioxide results (solid line).

TABLE I

Positions of maxima and minima on the energy scale for calculated Si K-EXAFS profiles compared with experimental results. * Two closed maxima or minima are treated together.

Si K-EXAFS profile	Position on the energy scale [eV]				
	min	max	min	max	min
Using input data [5, 6]		50	100	138	210
Using input data [11]	30	50	100*	155	242
This work	42*	84	148	201	284
Experiment [13]	50	86	142	211	288

5. Summary

We have theoretically obtained and analyzed K-EXAFS profiles for Si and O in silicon dioxide. Differences connected with amplitude of $\chi(k)$ function were observed between results for β-quartz and amorphous silicon dioxide. We have also noticed that Si K-EXAFS and O K-EXAFS profiles are out of phase for both forms. Our Si K-EXAFS results are in satisfactory agreement with experiment.

TABLE II

Positions of maxima and minima on the energy scale for calculated O K-EXAFS profiles compared with experimental results. * Two closed maxima or minima are treated together.

O K-EXAFS profile	Position on the energy scale [eV]			
	min	max	min	max
Using input data [5, 6]		42*	72	120
Using input data [11]		22	58	100
This work	22	56*	99	159
Experiment [12]	38	71	139	192

A significant improvement of our calculation in comparison to calculations based on the tabulated data has been observed. From the other hand, theoretical results for O K-EXAFS are in poor agreement with the experimentally obtained result, the discrepancy of 30 eV between theory and experiment can be seen. The simple model proposed by us gives better results than the tabulated data for silicon, but we ought to improve our treatment to obtain good results for oxygen. The most important difference between our calculations and calculations applied to obtain data [5, 6, 11] is that we have used ion wave functions for O^{-2} and Si^{+4}, while the neutral atom wave functions were used in above works. As we can see, it seems to be of importance.

References

[1] G.N. Greaves, *J. Non-Cryst. Solids* **71**, 203 (1985).

[2] G.E. Brown Jr., G.A. Waychunas, C.W. Ponader, W.E. Jackson, D.A. McKeown, *J. Phys. (France)* **47**, C8-661 (1986).

[3] J.B. Boyce, F. Bridges, T. Claeson, T.H. Geballe, *Phys. Rev. B* **39**, 11603 (1989).

[4] A. Krol, L.Y. Jang, S.C. Woronick, F. Xu, Y.D. Xao, Y.H. Kao, *Physica B* **158**, 465 (1989).

[5] A.G. Mc Kale, B.W. Veal, A.P. Paulikas, S.K. Chan, G.S. Knapp, *J. Am. Chem. Soc.* **110**, 3763 (1988).

[6] B.K. Teo, P.A. Lee, *J. Am. Chem. Soc.* **101**, 2815 (1979).

[7] J.J. Rehr, R.C. Albers, C.R. Natoli, E.A. Stern, *Phys. Rev. B* **34**, 4350 (1986).

[8] A. Balerna, M. Benfatto, S. Mobilio, C.R. Natoli, A. Filipponi, F. Evangelisti, *J. Phys. (France)* **47**, C8-63 (1986).

[9] P.A. Lee, G. Beni, *Phys. Rev. B* **15**, 2862 (1977).

[10] D.E. Sayers, B.A. Bunker, *X-ray Applications. Principles. Applications. Technique of EXAFS, SEXAFS, XANES*, Eds. D.C. Koningsberger, R. Prins, Wiley, New York 1988.

[11] J. Mustre de Leon, J.J. Rehr, S.I. Zabinsky, *Phys. Rev. B* **44**, 4146 (1991).

[12] J. Stohr, L. Johansson, I. Lindau, P. Pianetta, *Phys. Rev. B* **20**, 664 (1979).

[13] G.N. Greaves, A. Fontaine, P. Lagarde, D. Raoux, S.J. Gurman, *Nature* **293**, 611 (1981).

[14] W.L. Schaich, in: *EXAFS and Near Edge Structure III,* Eds. K.O. Hodgson, B. Hedman, J.E. Penner-Hahn, Springer Verlag, Berlin 1984.

[15] J.J. Barton, D.A. Shirley, *Phys. Rev. B* **32**, 1892 (1982).

[16] P.A. Lee, J.B. Pendry, *Phys. Rev. B* **11**, 2795 (1975).

[17] W.Y. Ching, *Phys. Rev. B* **26**, 6610 (1982).

[18] E. Heinninger, R.C. Buschert, *J. Phys. Chem. Solids* **28**, 423 (1967).

[19] E. Clementi, C. Roetti, *At. Data Nucl. Data Tables* **14**, 177 (1979).

[20] J.B. Pendry, *Low Energy Electron Diffraction,* Academic Press, London 1974.